

Journal of Materials Science: Materials in Medicine

Laser surface alloying of 316 L stainless steel coated with a bioactive hydroxyapatite-titanium oxide composite

--Manuscript Draft--

Manuscript Number:	JMSM6430R2
Full Title:	Laser surface alloying of 316 L stainless steel coated with a bioactive hydroxyapatite-titanium oxide composite
Article Type:	S.I. : MiMe conference 2013
Corresponding Author:	El-Sayed Ghaith, PhD Teesside University Middlesbrough, UNITED KINGDOM
Corresponding Author Secondary Information:	
Corresponding Author's Institution:	Teesside University
Corresponding Author's Secondary Institution:	
First Author:	El-Sayed Ghaith, PhD
First Author Secondary Information:	
Order of Authors:	El-Sayed Ghaith, PhD El-Sayed Ghaith, PhD Simon Hodgson Martin Sharp
Order of Authors Secondary Information:	
Abstract:	Laser surface alloying (LSA) is a powerful technique for improving the mechanical and chemical properties of engineering components. In this study, Laser surface irradiation process employed in the surface modification off 316 L stainless steel substrate using hydroxyapatite-titanium oxide to provide a composite ceramic layer for the suitability of applying this technology to improve the biocompatibility of medical alloys and implants. Fusion of the metal surface incorporating hydroxyapatite-titania ceramic particles using a 30 W Nd:YAG laser at different laser powers, 40 %, 50% and 70 % power and a scan speed of 40 mms ⁻¹ was observed to adopt the optimum condition of ceramic deposition. Coatings were evaluated in terms of microstructure, surface morphology, composition biocompatibility using XRD, ATR-FTIR, SEM and EDS. Evaluation of the in vitro bioactivity by soaking the treated metal in SBF for 10 days showed the deposition of biomimetic apatite.
Response to Reviewers:	All fingers comments have been done. Thank you

Laser surface alloying of 316 L stainless steel coated with a bioactive hydroxyapatite-titanium oxide composite

El-Sayed Ghaith^{1,2}, Simon Hodgson¹ and Martin Sharp³

¹*School of Science and Technology, Teesside University, Middleborough, TS1 3BA, UK*

²*Zagazig University, Egypt*

³*General Engineering Research Institute, Liverpool John Moores University, Byrom Street, Liverpool L3 3AF, UK*

Corresponding author: E.ghaith@tees.ac.uk

Keywords: Sol-gel, Coating, Laser surface alloying, Titanium oxide, Hydroxyapatite.

Abstract

Laser surface alloying (LSA) is a powerful technique for improving the mechanical and chemical properties of engineering components. In this study, Laser surface irradiation process employed in the surface modification of 316 L stainless steel substrate using hydroxyapatite-titanium oxide to provide a composite ceramic layer for the suitability of applying this technology to improve the biocompatibility of medical alloys and implants. Fusion of the metal surface incorporating hydroxyapatite-titania ceramic particles using a 30 W Nd:YAG laser at different laser powers, 40 %, 50% and 70 % power and a scan speed of 40 mm^s⁻¹ was observed to adopt the optimum condition of ceramic deposition. Coatings were evaluated in terms of microstructure, surface morphology, composition biocompatibility using XRD, ATR-FTIR, SEM and EDS. Evaluation of the *in vitro* bioactivity by soaking the treated metal in SBF for 10 days showed the deposition of biomimetic apatite.

Introduction

Laser processing has been extensively applied in the surface modification of metals and alloys as an alternative approach for the conventional heating techniques to produce functional ceramic coatings on the metals/alloy surface [1]. Due to many advantages, such as tailored mechanical and chemical

1 properties short processing time, fast heating/cooling rate, low energy consumption, localised heating
2 and accurate control over the process and environmentally friendly technology [1-4] this process has
3 been widely used in the recent decade. Moreover, laser surface modification as a beneficial tool to
4 modify the surface properties of the metallic substrates, without affecting the bulk properties of the
5 substrate meanwhile generating of meta-stable structures with novel properties that not achieved by
6 competing methods [1-2].

7 Laser surface alloying and modification is carried out by impinging the laser energy on the substrate
8 concomitant with the addition of the desired materials.

9 The sol-gel coating method has been shown to be a useful technique to produce bulk, powder, and
10 coated film ceramic materials. It has also been used in the syntheses of amorphous and/or crystalline
11 oxides as well as ceramic coatings. The advantages of the sol-gel method over other coating
12 techniques include its excellent adhesion to substrates, lower processing temperatures, corrosion
13 protection, as well as the production of high quality coatings and high purity products [3-5].

14 Laser irradiation process has been employed in some cases to induce calcination of the sol-gel
15 coatings in order reduce the influence of heat or plasma on the bulk structure and properties of the
16 metals. In our earliest work, CO₂ laser and Nd:YAG laser have been used to crystallise titanium
17 oxide thin film deposited on a glass substrate [6-7]. Winfield et al. [8] used excimer laser to
18 crystallise zinc oxide thin films prepared by sol-gel technique. Starbova et al. [9] investigated effects
19 of excimer laser irradiation on the structure and performance of sol-gel titanium oxide films.
20 Adraider et al. applied the laser processing of Al₂O₃, ZrO₂, TiO₂ sol-gel coatings on the surface
21 modification of stainless steel for engineering applications [10-12]. Therefore, the combination of
22 sol-gel coating and laser processing for surface modification is of great interest due to the suitability
23 of both technologies for processing mechanically stable thin film materials.

24 316L Stainless steel is among the most commonly used materials in biomedical implantations.
25 Biocompatibility plays a crucial role in implant fixation and bone cell adherence is associated with

1 the surface topography, energy and roughness. However, 316L stainless steel cannot meet all the
2 clinical requirements; in order to be successfully used as biocompatible implants for hard tissue
3 replacement they must be bonded to the surrounding bone tissue. Coating the implant with a
4 bioactive ceramic or glass-ceramic layer has been reported to show good fixation to the host bone
5 and to lead to an increase in bone growth to the implant [13-14].
6
7
8
9
10

11 The aim of this work is the use of a combined sol-gel-laser rapid prototyping process for the
12 fabrication of high mechanical stable bioactive titania-hydroxyapatite metal matrix composite
13 (MMC) layer on the surface of the 316L stainless steel. The process could offer a high rate of
14 bioactivity compared with the pure titanium oxide due to incorporating a small amount of
15 hydroxyapatite powder into a titania sol. The injected particles do not decompose under the influence
16 of laser power and remain embedded in the matrix of the substrate to yield a MMC layer (consisting
17 of a hydroxyapatite-titanium oxide-metal composite) which could be extremely promising in
18 bioactive surface modification of biomedical implants.
19
20
21
22
23
24
25
26
27
28
29
30
31

32 **2. Materials and Methods**

33 **2.1. Sample preparation**

34 Nano-size hydroxyapatite powder purchased from Sigma-Aldrich, UK, was added by weight (7.5 Wt
35 %) into a pre-hydrolysed titania sol in ultrasonic bath. The titania sol was obtained by hydrolysis of
36 titanium (IV) n-butoxide with water at room temperature in the presence of acetyl acetone as a
37 chelating agent and ethanol as a solvent. The molar ratio was maintained at a ratio of 1:1:26.5:1
38 titanium (IV) n-butoxide:acetyl acetone:ethanol:water [7].
39
40
41
42
43
44
45
46
47
48
49
50
51

52 The chemical composition of the stainless steel, stainless steel 316L substrates is shown in Table 1.
53 The metal substrates were cut into small square plates of 50×25 mm with a thickness of 3 mm,
54 polished through different stages to give the surface a mirror finish before washing with detergent
55 and electrical cleaning in a chemical solution, followed by rinsing with deionised water and alcohol
56
57
58
59
60
61
62
63
64
65

1 and drying in air before use. The cleaned substrates were coated with hydroxyapatite-titania sol (HA-
2 titania).
3

4
5 The HA-titania composite sol was applied under wet conditions onto the metal surface and laser
6 scanned using a 30 W Nd:YAG laser tuned to a wavelength of 1064 nm at 40%, 50% and 70% laser
7 power scanned at 40 mms⁻¹ and operated in continuous wave mode (CW). The laser beam spot
8 diameter of 23 μm was focused and laser scan covers a rectangle of 10 x 10 mm with a distance of
9
10
11
12
13
14
15
16
17
18
19
20
21
22
23
24
25
26
27
28
29
30
31
32
33
34
35
36
37
38
39
40
41
42
43
44
45
46
47
48
49
50
51
52
53
54
55
56
57
58
59
60
61
62
63
64
65

The laser energy densities were calculated with equation (1) and are presented in Table 1.

$$E = P/(v \cdot D) \quad \text{Eq. (1)}$$

Where, E is the energy density (J mm⁻²); P is the average laser power (W); v is traverse speed (mm⁻¹); and D is focussed beam spot diameter (μm).

The experimental set-up is shown in Figure 1. The substrate was fixed inside the laser machine on an X-Y stage, the prepared sol applied to its surface, and laser irradiation performed immediately while the sol was still wet during laser irradiation. The laser was operated through a computer programmed X-Y scanning process to cover an area of 10×10 mm square.

2.2. Biological testing

The apatite formation was examined by soaking the sample in simulated body fluid (SBF, 50 mL) for 10 days at 37 °C and a pH of 7.40. The composition of this buffer, described by Kokubo and was prepared by dissolving analytical grade reagent of NaCl, NaHCO₃, KCl, K₂HPO₄·3H₂O, MgCl₂·6H₂O, CaCl₂ and Na₂SO₄ in Milli-Q water and at the solution pH kept at 7.40 with tris (hydroxymethyl) aminomethane ((CH₂OH)₃CNH₂) and an appropriate amount of aqueous HCl solution. The inorganic ion concentrations is Na⁺142.0; K⁺ 5.0; Mg²⁺ 1.5; Ca²⁺ 2.5; Cl⁻ 147.8; HCO₃⁻ 4.2; HPO₄²⁻ 1.0; and SO₄²⁻ 0.5 mol/m³, pH 7.40 which is nearly equal to those of human

1 blood plasma at 37.0 °C. Samples were removed from SBF after a given period, rinsed with ultra-
2 pure water, and then dried at room temperature [15].
3
4
5
6

7 **2.3. Characterisation**

8
9

10 The X-ray diffraction (XRD) analysis was conducted using a Siemens D500 diffractometer with
11 CuK α radiation at 20 mA and 40 kV. The diffraction spectrum was recorded in the range of 2 θ from
12 20° to 60° at a step size of 0.02° and step time of 1 s. The analysis of attenuated total reflectance
13 Fourier transform infrared spectroscopy (ATR-FTIR) was carried out on a Thermo Nicolet 5700
14 FTIR spectrometer. All spectra were recorded over the range 400–4000 cm⁻¹ at a resolution of 4
15 cm⁻¹ averaged over 32 scans. Coated substrate samples were used directly and analysed without
16 additional preparation [6].
17
18
19
20
21
22
23
24
25
26

27 The microstructure and surface morphology of the coated samples before and after soaking in SBF
28 were observed using a scanning electron microscope (SEM, Hitachi 3400 N, Japan) incorporating X-
29 ray microanalysis using energy dispersive spectroscopy (EDS) using INCA software (Oxford
30 Instruments, UK).
31
32
33
34
35
36

37 The adhesive strength of the deposited layer was evaluated by a tape-test method (D 3359-02 ASTM
38 standard) according to Scotch 810-1-12C.
39
40
41
42

43 **Results and Discussions**

44

45 **3.1. Surface morphology**

46
47

48 The surface morphology of the laser-deposited hydroxyapatite-titania film on stainless steel
49 substrates was observed using scanning electron microscopy to study the effect of laser energy
50 densities on the morphology of substrate surface at a micro-scale. Figure 2 shows the SEM
51 micrographs revealing the surface morphologies of coated 316L stainless steel. At the lower energy
52 density (13.04 J mm⁻¹), the surface has no deposition of hydroxyapatite-titania. It displays scattered
53
54
55
56
57
58
59
60
61
62
63
64
65

1
2
3
4
5
6
7
8
9
10
11
12
13
14
15
16
17
18
19
20
21
22
23
24
25
26
27
28
29
30
31
32
33
34
35
36
37
38
39
40
41
42
43
44
45
46
47
48
49
50
51
52
53
54
55
56
57
58
59
60
61
62
63
64
65

dry particles as shown in Figure (2-A) sample-1. Increasing the power density into 16.30 J mm⁻¹ Figure 2-B (sample-2) has not shown any significance difference from sample-1. Further increasing the power density by changing the laser power, the coating deposited at 20.83 J mm⁻¹ (sample 3) Figure 2-C shows a rough surface morphology composed of grains fused together with the metal surface, which is metal ceramic matrix. These micrographs highlight a heterogeneous surface with depositions of differently sized spherical particles consisting of blended hydroxyapatite-titanium oxide composite. The particle size ranges from sub microns to several microns. Figure 3-A (higher magnification of C) shows fusion of the ceramic coating and imbedded into the metal surface. Table 3 represents results of EDS analysis of the coated surface. Results demonstrate the a sharp decrease in elements Fe (from 65.00% to 4.67%) , Cr (from 16.00% to 3.26%) and Ni (from 10.00 % to 1.21 %) associated with the 316L substrate due to surface coatings. While peaks corresponding to Ti (65.47%), Ca (12.83%) and P (9.07%) consistent with the elements associated with the presence of hydroxyapatite-titania coatings. Ti peaks are shown due to the deposition (crystallisation) of titanium oxide. These results suggest that the metal surface was fused due to the thermal effect of the laser power; the titania sol appears to be crystallised and blended with hydroxyapatite to form apatie-TiO₂ spheres which are embedded into the metal surface matrix [6-13, 17]. This indicates that the laser energy density plays the major role for the deposited coating thickness.

Additionally, Figure 3-B shows the highest magnification of the coated metal surface. The images display the variation in both morphology and composition of the surface; the EDS spectrum collected from the large particles reveal slightly higher phosphorus content than the surrounding. This is probably attributable to decomposition of some hydroxyapatite into calcium oxide under the thermal effects of the laser [6-12].

The results show that increases in the laser power at the same traverse speed leads to increase of the rate of deposition than the low laser power and the presence of more titania and hydroxyapatite. The

1 effect of the laser power is related to the energy delivered to the scanned area by the laser beam. The
2 higher the laser power leads to increasing the laser energy density hence increase the rate of
3 hydroxyapatite-titania depositions and increase the amount off Ti, Ca and P ions to be detected my
4 EDS. At the same time the amount of iron detected is decreased due to increasing of the coating
5 thickness. While at lower power and low no noticeable depositions of the material on the surface of
6 the metal have been observed.
7
8
9
10
11
12
13
14

15 Figure 4 shows the cross-sectional image and EDS spectrum of the laser deposited hydroxyapatite -
16 titania coatings on steel substrate at 22.83 J mm^{-1} and the measurements of the coating thickness. The
17 coating thickness is about $9 \mu\text{m}$ at the applied laser conditions.
18
19
20
21

22 Figure 5 shows the SEM micrographs and the EDS spectrum collected from the coated 316 L SS
23 after soaking in SBF for 10 days. It can be seen that biomimetic apatite is spontaneously formed on
24 the metal surface. The Ca/P molar ratio consistent with about 1.6 is observed from EDS analysis
25 after 10 days of immersion in SBF, which implies that the surface is bioactive and the hydroxyapatite
26 did not decompose under the influence of the laser treatment. However, samples soaked for 5 days
27 did not show any new apatite formation (data not shown). This may be due to the fusion process,
28 which might retard the Ca^{2+} ion release [6,13-17].
29
30
31
32
33
34
35
36
37
38
39

40 The formation of biomimetic apatite is attributed to the migration (release) of Ca^{2+} ions from the
41 coated metal surface forming a saturated solution with respect to apatite. Ca^{2+} ions react with $(\text{PO}_4)^{3-}$
42 forming amorphous CaP. In the meantime, titania on the coated metal surface reacts with H_3O^+ from
43 the SBF forming a hydrated Ti-OH rich surface attracting the CaP and inducing apatite nucleation.
44 Hence, crystallization of the amorphous CaP occurred by incorporation of OH^- and CO_3^{2-} ions from
45 the solution to from the apatite layer [5-6,13-17].
46
47
48
49
50
51
52
53
54

55 3.3. X-ray diffraction analysis and ATR-FTIR analysis 56 57 58 59 60 61 62 63 64 65

1 Figure 6 shows XRD patterns collected from the film surfaces. The data illustrate the peaks at 2θ at
2 25.30° and 36° corresponding to the crystallization of titania into anatase crystals. Peaks relating to
3 hydroxyapatite are seen at 2θ , 26.00° and 32.00°. The two high intensity diffraction peaks at 2θ =
4 43.7° and 50.3° were recorded which are attributed to the diffractions of the substrate [9,13-17].
5
6
7
8
9

10 The effect of Nd:YAG laser irradiation on the chemical composition of the deposited layer has been
11 investigated using ATR-FTIR spectroscopy. Figure 7 shows the spectrum collected from the laser
12 irradiated area showing high strong absorption band at 1036 cm^{-1} which is attributed to the $(\text{PO}_4)^{3-}$
13 group. Similarly, the absorption bands at 1090 cm^{-1} and 965 cm^{-1} are assigned to $(\text{PO}_4)^{3-}$. The band
14 observed at 1432 cm^{-1} and 1550 cm^{-1} is due to the vibrations of the bonds within the CO_3^{2-} group
15 which are attributable to the apatite crystal lattice and calcium carbonate [7,11]. The absorption band
16 (small shoulder) at 650 cm^{-1} is indicative of the Ti–O–Ti vibration [10]. These results suggest that
17 the ATR-FITR and XRD data are consistent.
18
19
20
21
22
23
24
25
26
27
28
29

30 **3.4 Mechanical stability**

31 The mechanical stability of the titania-hydroxyapatite coating to the steel substrate was employed to
32 determine the adhesion strength. The coated metal surface before and after the adhesion test has been
33 investigated using SEM. Figure 8 (A,B) shows the SEM micrographs of the coated steel substrate
34 before and after the adhesion by applying the tape test method. According to the SEM micrographs,
35 the analysis of the surface reveals that no debonding of the titania-hydroxyapatite layer from the
36 substrate. Thus, these results prove of good bond strength of the titania-hydroxyapatite coatings to
37 L316 steel substrate due to surface fusion of the metal and the ceramic coating.
38
39
40
41
42
43
44
45
46
47
48
49

50 **Conclusion**

51 Bioactive hydroxyapatite-titania coatings have been successfully deposited and embedded onto a
52 316L steel substrate surface by means of a combined laser-sol–gel technique for laser surface
53 alloying, with laser irradiation of wet sol–gel coatings requiring the following application: 30 W
54 Nd:YAG laser tuned to 1064 nm, 21 power, 40 mms^{-1} scan speed and continuous wave mode. The
55
56
57
58
59
60
61
62
63
64
65

1 resulted coatings are strongly bonded to the steel surface. Accordingly, laser-irradiation heats some
2 materials containing water; water in sol-gel derived materials absorbs laser energy resulting in
3 conversion into heat energy. Nd:YAG laser-irradiation of sol-gel derived titanium oxide containing
4 small ratio of hydroxyapatite powder resulted in the crystallization of anatase form alongside the
5 hydroxyapatite and both fused into the surface of the steel substrate under the action of high laser
6 power..
7
8
9
10
11
12
13
14

15 The biomimetic apatite was formed on the surface after a period of 10 days soaking in simulated
16 body fluid (SBF), at 37 °C and a pH of 7.40, indicating an improvement in biocompatibility resulting
17 from the modified 316L stainless steel surface.
18
19
20
21
22

23 **Acknowledgments**

24
25

26 The author thanks the staff at Lairdsie Engineering Centre, University of Liverpool for supporting
27 this work and to The University of Liverpool for providing the essential laser facilities
28
29
30
31
32
33
34
35
36
37
38
39
40
41
42
43
44
45
46
47
48
49
50
51
52
53
54
55
56
57
58
59
60
61
62
63
64
65

References

- [1] S Bandyopadhyay, J.K Sarin Sundar, G.Sundararajan, S.V Joshi. Journal of Materials Processing Technology, Vol. 127, 1, (2002), p. 83.
- [2] A. Viswanathan, D. Sastikumar. Optics and Laser Technology, Vol. 39 (2007), p. 1504.
- [3] J. Gallardo, P. Galliano and A. Duran: Journal of Sol-Gel Science and Technology, Vol. 21 (2001), p. 65.
- [4] Bing Su, Guoqing Zhang, Xudong Yu, Chengtao Wang. Journal of University of Science and Technology Beijing, Mineral, Metallurgy, Material, Volume 13, Issue 5, (2006), p. 469.
- [5] J. Harle, Hae-Won Kim, N. Mordan, J. Knowles, V. Salih. Acta Biomaterialia, Volume 2, Issue 5, (2006), p. 547.
- [6] E.-S Ghaith, T. Hayakawa, T. Kasuga, and M. Nogami. Journal of Materials Science, 41[8] (2006), p. 2521.
- [7] E.-S. Ghaith, T. Hayakawa, T. Kasuga and M. Nogami: Materials letter, Vol. 60 (2006), p. 194.
- [8] R.J. Winfield, L.H.K. Koh, S, O'Brien, and G. M. Crean, Appl. Surf. Sci. 254 (2007), p. 855.
- [9] K. Starbova, V. Yordanova, D. Nihtianova, W. Hintz, J. Tomas, N. Starbov, Appl. Surf. Sci. 254 (2008), p. 4044.
- [10] Y. Adraider, Y.X. Pang, F. Nabhani, S.N. Hodgson, Z.Y. Zhang Surface & Coatings Technology 205 (2011), p. 5345.
- [11] Y. Adraider, Y.X. Pang, M.C. Sharp, S.N. Hodgson, F. Nabhani, A. Al-Waidh, Materials Chemistry and Physics 138 (2013), p. 245.
- [12] Y. Adraider, Y.X.Pang, F.Nabhani, S.N.Hodgson, M.C. Sharp, A.Al-Waidh Ceramics International 39(2013), p. 9665.

- 1
2
3 [13] M.H. Fathi and A.D. Mohammadi, *Materials Science and Engineering A*, Vol. 474, Issue 1-2,
4
5 (2007) p.128.
6
7
8 [14] A. Balamurugan, G. Balossier, S. Kannan, J. Michel, A. Robelo and J. Ferrira, *Acta*
9
10 *Biomaterialia*, Vol. 3 (2007), p.255.
11
12
13 [15] T. Kokubo and H. Takamada: *Biomaterials*, Vol. 27 (2006), p. 2907.
14
15
16 [16] L. Hench and D. Clark, *Journal of Non-Crystalline Solids*, Vol. 28 (1978), p. 83.
17
18
19 [17] K. Starbova, V. Yordanova, D. Nihtianova, W. Hintz, J. Tomas, N. Starbov, *Appl. Surf.*
20
21 *Sci.*, Vol. 254 (2008), p.4044.
22
23
24 [18] T. Ezz, P. Crouse, L. Lin, Z. Liu, *Surface Coating Technology*, Vol. 200 (2006), p.6395.
25
26
27 [19] A.J. Lopez, A. Urena, J. Rams, *Surface Coating Technology*, Vol. 203 (2009), p. 1474.
28
29
30 [20]H.W. Kim,Y.H.Koh,L.H.Li,S.Lee,H.W.Kim, *Biomaterials*, Vol. 25 (2004), p. 2533.
31
32
33 [21] W. Pon-On, N. Charoenphandhu I-M. Tang, J. Teerapornpuntakit, J. Thongbunchoo, N.
34
35
36 *Krishnamra Materials Science and Engineering C*, Vol. 33 (2013), p. 251.
37
38
39
40
41
42
43
44
45
46
47
48
49
50
51
52
53
54
55
56
57
58
59
60
61
62
63
64
65

Table 1. Chemical composition of the 316L stainless steel substrate used.

%C	%Mn	%Si	%P	%S	%Cr	%Mo	%Ni	%N	%Fe
0.08	2.0	0.75	0.045	0.03	16.0–18.0	2.0–3.0	10.0–14.0	0.1	65.0

Table 2. Laser conditions for hydroxyapatite-titania coating.

Sample	Laser conditions		
	Power (W)	Traverse speed mms^{-1}	Energy density J mm^{-2}
1	12	40	13.04
2	15	40	16.30
3	21	40	22.83

Table 3. EDS analysis of the major elements (atomic %) of 316L steel substrate after coating with hydroxyapatite-titania.

% Ca	% P	%Mn	%Ni	%Ti	%S	%Cr	%Mo	%Ni	%Fe
12.83	9.07	0.75	1.21	65.47	1.10	3.26	1.12	0.52	4.67

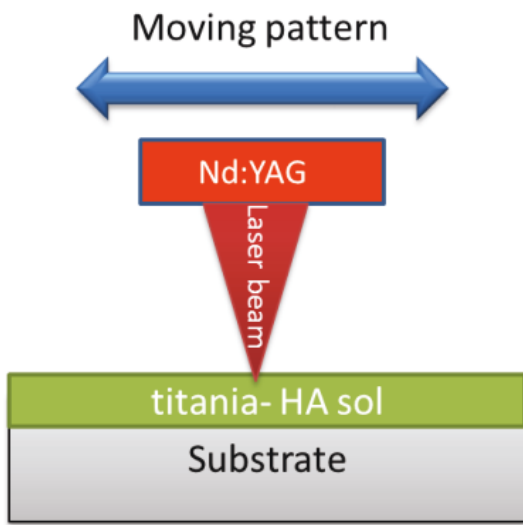


Figure 1: Schematic setting of laser surface alloying procedure.

1
2
3
4
5
6
7
8
9
10
11
12
13
14
15
16
17
18
19
20
21
22
23
24
25
26
27
28
29
30
31
32
33
34
35
36
37
38
39
40
41
42
43
44
45
46
47
48
49
50
51
52
53
54
55
56
57
58
59
60
61
62
63
64
65

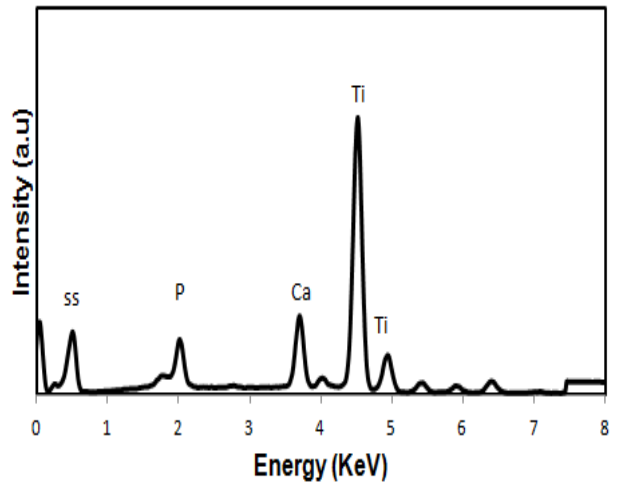
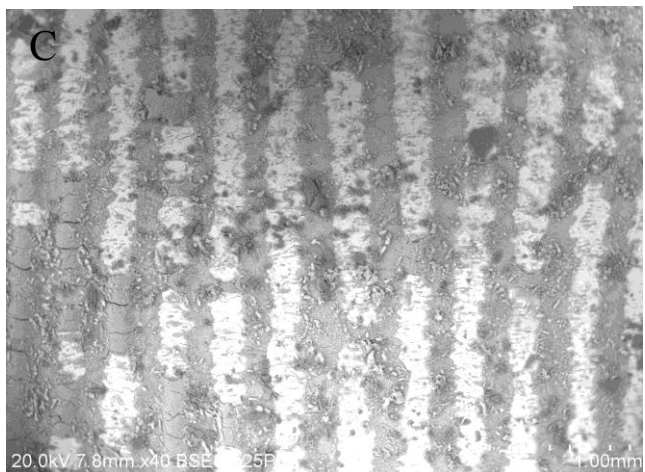
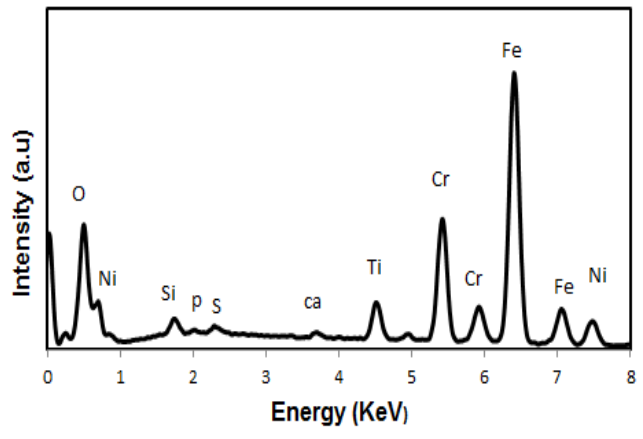
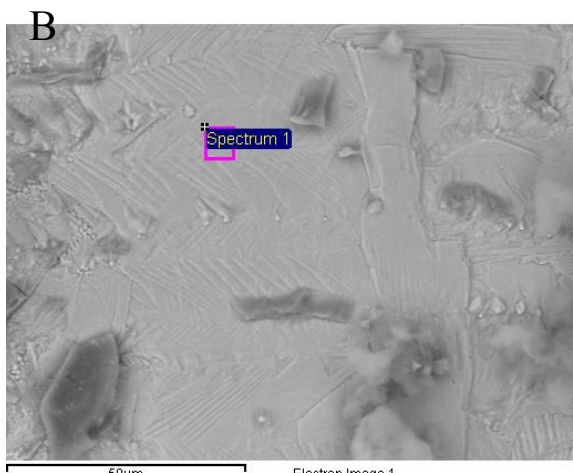
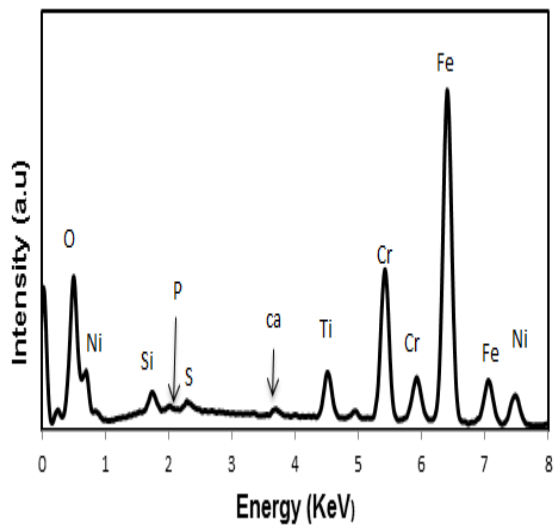
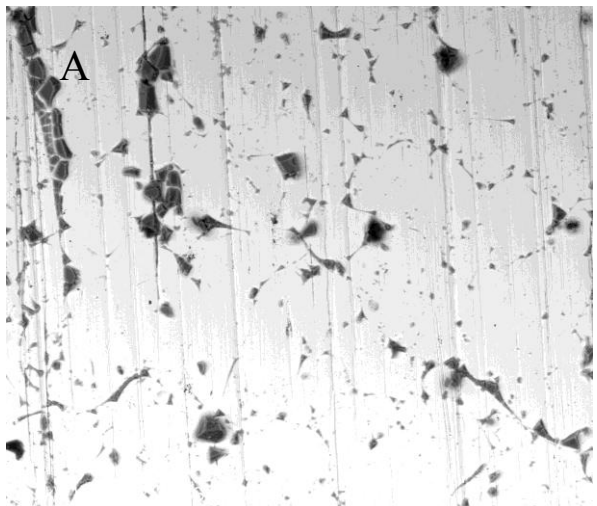


Figure 2. SEM micrographs of the laser irradiate steel substrates at different laser energy densities.

1
2
3
4
5
6
7
8
9
10
11
12
13
14
15
16
17
18
19
20
21
22
23
24
25
26
27
28
29
30
31
32
33
34
35
36
37
38
39
40
41
42
43
44
45
46
47
48
49
50
51
52
53
54
55
56
57
58
59
60
61
62
63
64
65

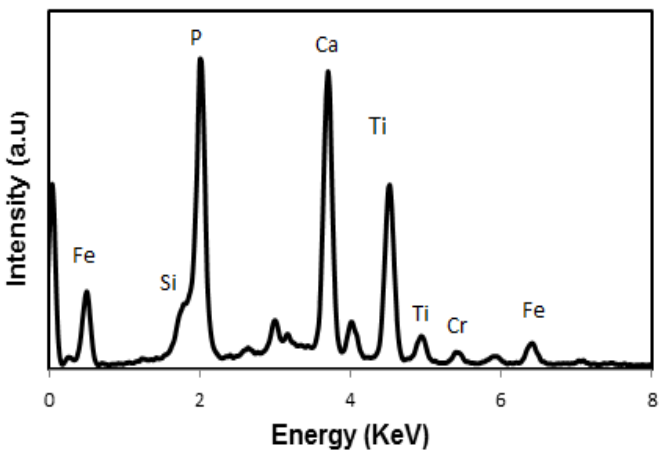
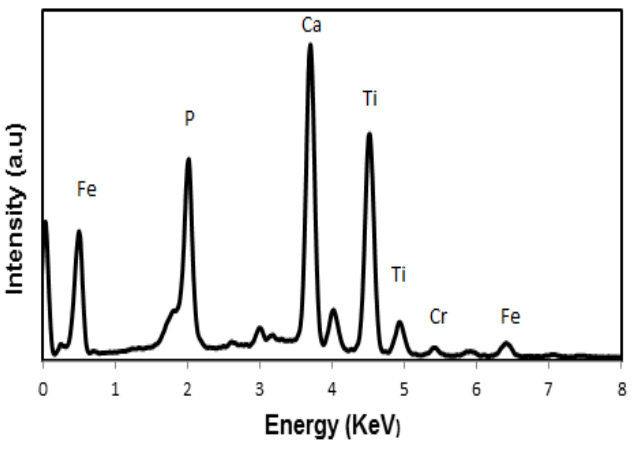
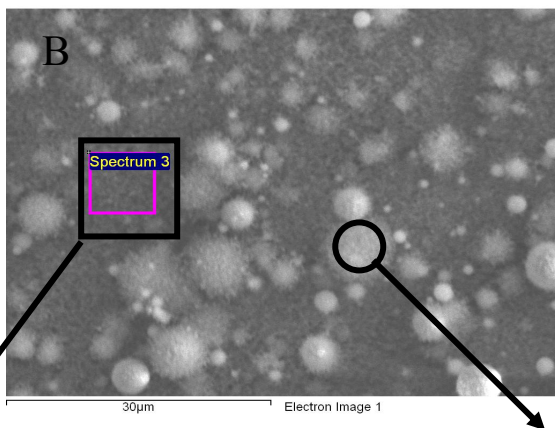
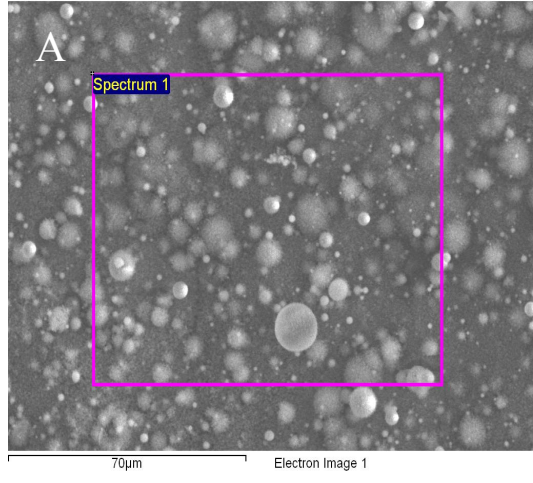
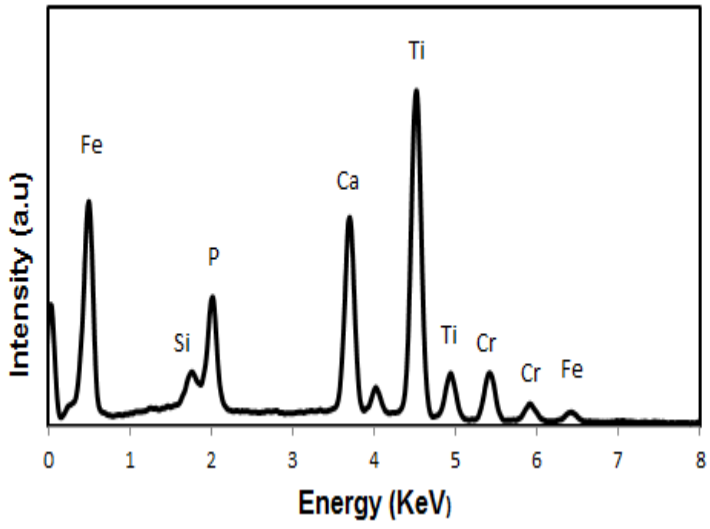


Figure 3. SEM micrographs of the 316L stainless steel substrate after laser surface alloying (LSA) using Nd:YAG laser at 70 % laser power output of 30 W.

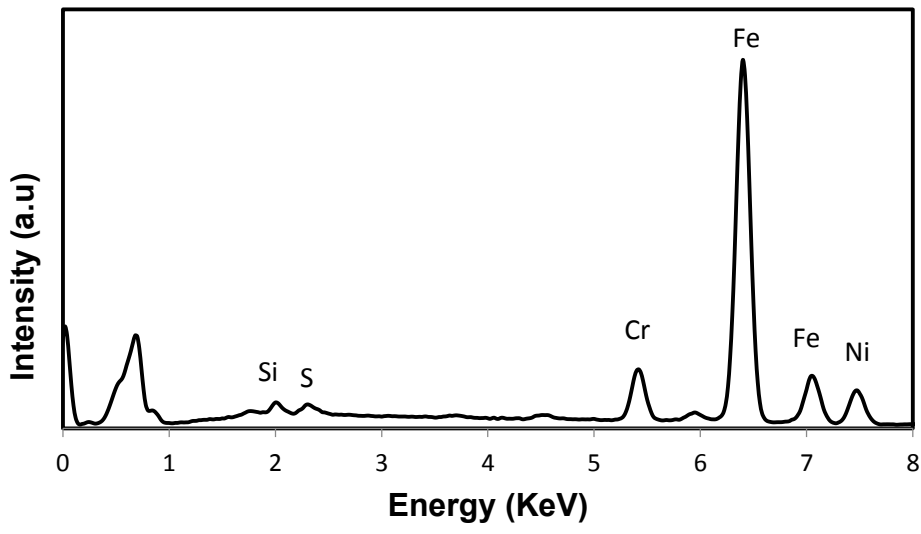
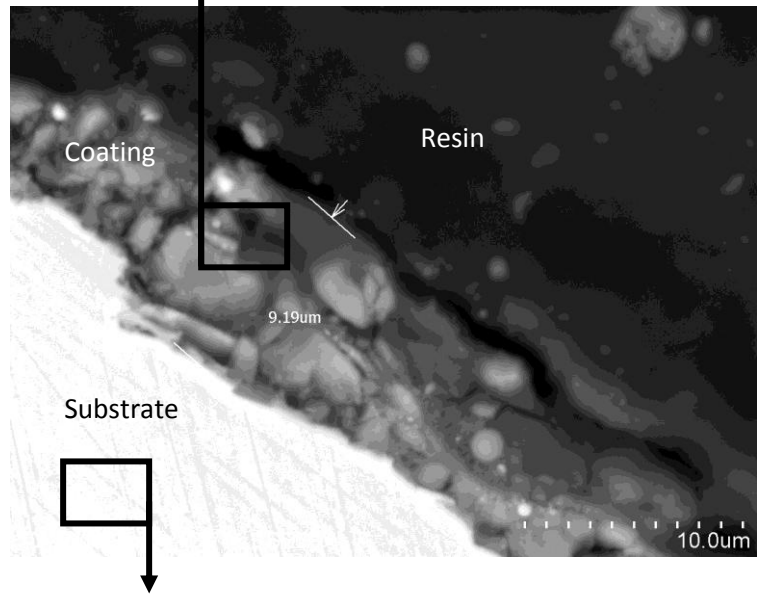
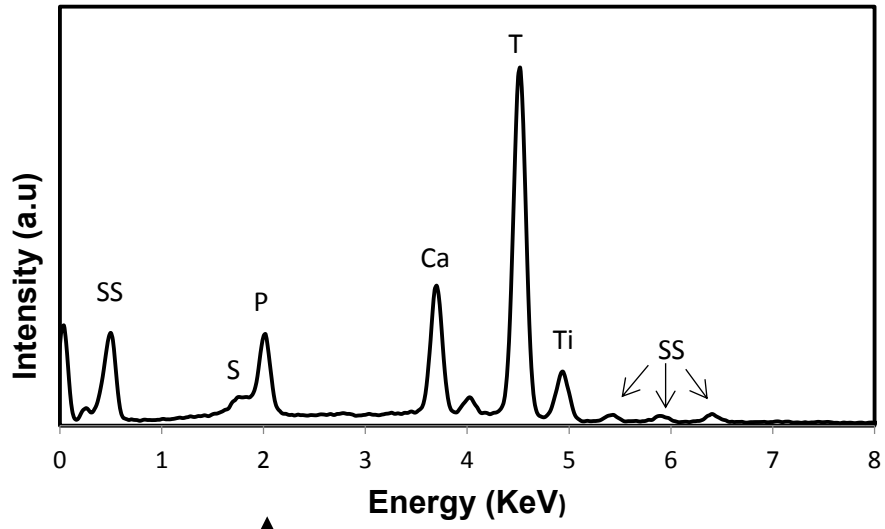


Figure 4. SEM images of the cross section and related EDS of hydroxyapatite-titania coating deposited on L316 steel substrate.

1
2
3
4
5
6
7
8
9
10
11
12
13
14
15
16
17
18
19
20
21
22
23
24
25
26
27
28
29
30
31
32
33
34
35
36
37
38
39
40
41
42
43
44
45
46
47
48
49
50
51
52
53
54
55
56
57
58
59
60
61
62
63
64
65

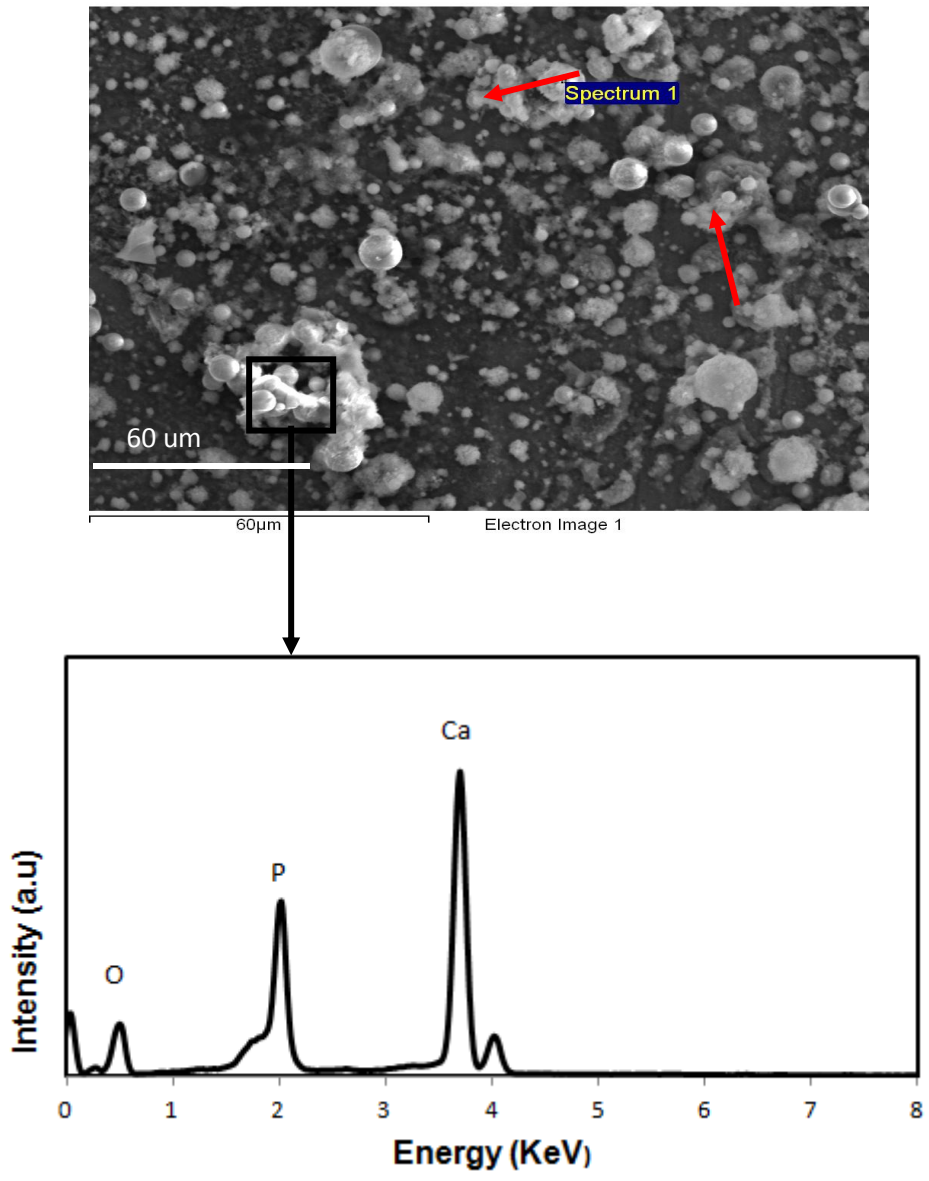


Figure 5. SEM micrographs of the stainless steel (316L) substrate coated with hydroxyapatite-titanium oxide composite after soaking in SBF for 10 days (the arrows refer to newly formed apatite).

1
2
3
4
5
6
7
8
9
10
11
12
13
14
15
16
17
18
19
20
21
22
23
24
25
26
27
28
29
30
31
32
33
34
35
36
37
38
39
40
41
42
43
44
45
46
47
48
49
50
51
52
53
54
55
56
57
58
59
60
61
62
63
64
65

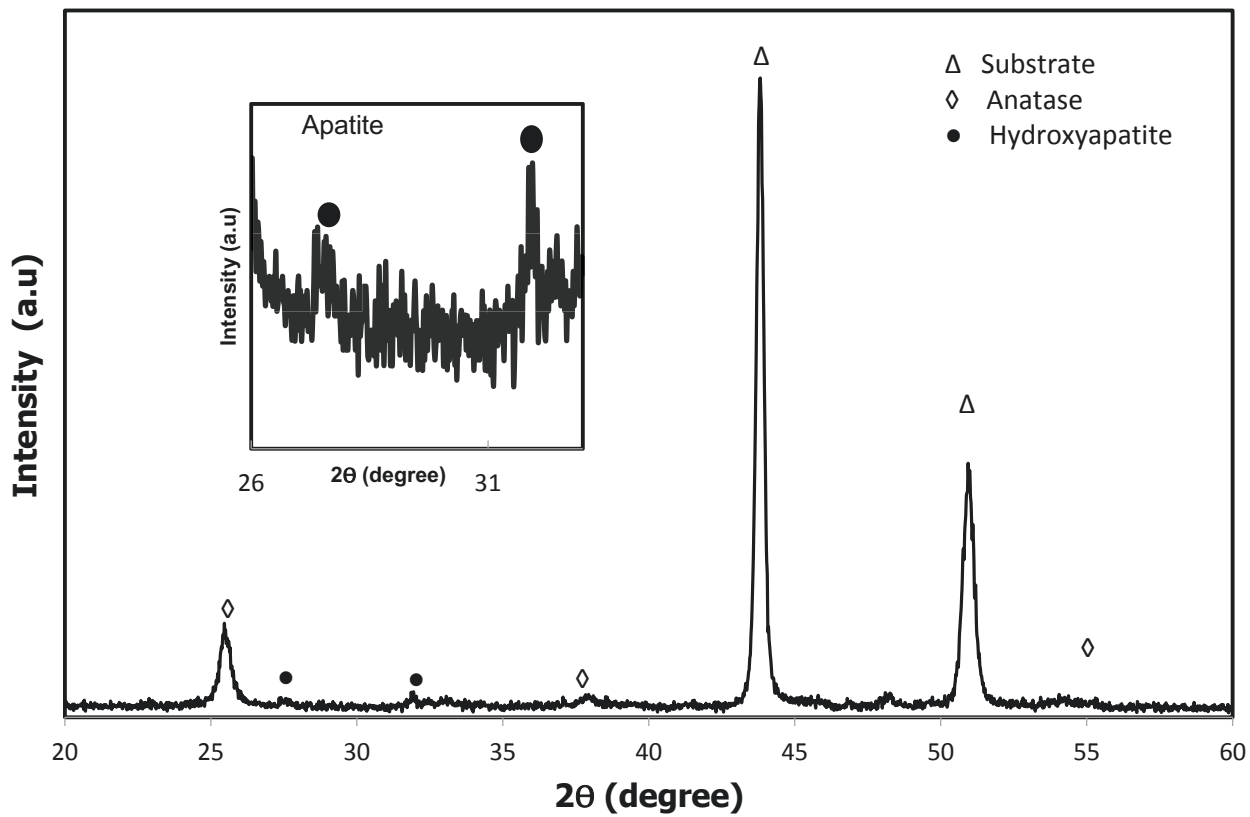


Figure 6. XRD patterns of sol-gel hydroxyapatite-titania coatings on steel substrate.

1
2
3
4
5
6
7
8
9
10
11
12
13
14
15
16
17
18
19
20
21
22
23
24
25
26
27
28
29
30
31
32
33
34
35
36
37
38
39
40
41
42
43
44
45
46
47
48
49
50
51
52
53
54
55
56
57
58
59
60
61
62
63
64
65

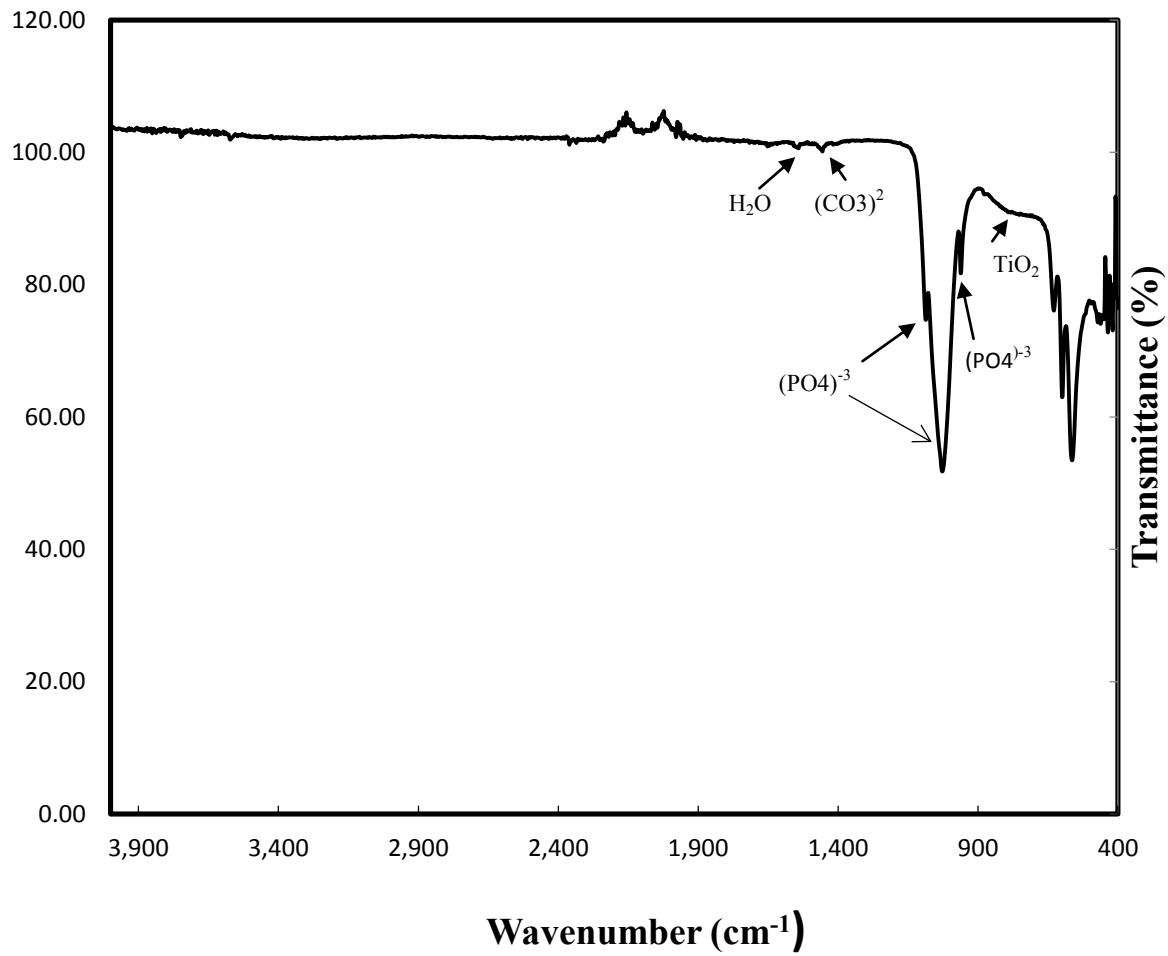


Figure 7. FTIR spectrum of the laser-deposited sol-gel titania-hydroxyapatite coating on 316L steel substrate.

1
2
3
4
5
6
7
8
9
10
11
12
13
14
15
16
17
18
19
20
21
22
23
24
25
26
27
28
29
30
31
32
33
34
35
36
37
38
39
40
41
42
43
44
45
46
47
48
49
50
51
52
53
54
55
56
57
58
59
60
61
62
63
64
65

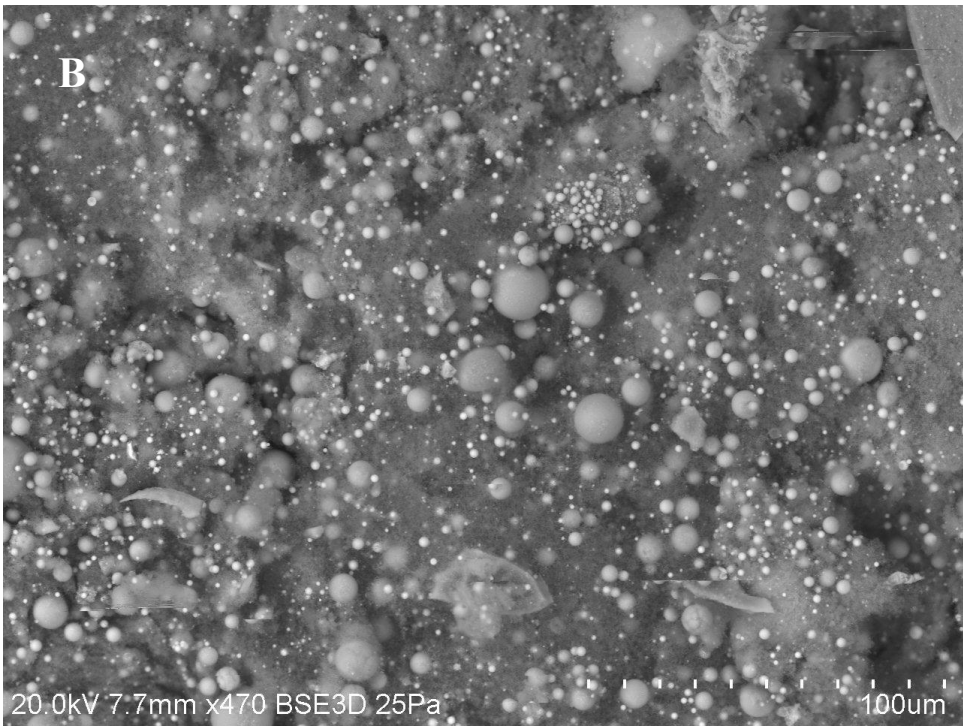
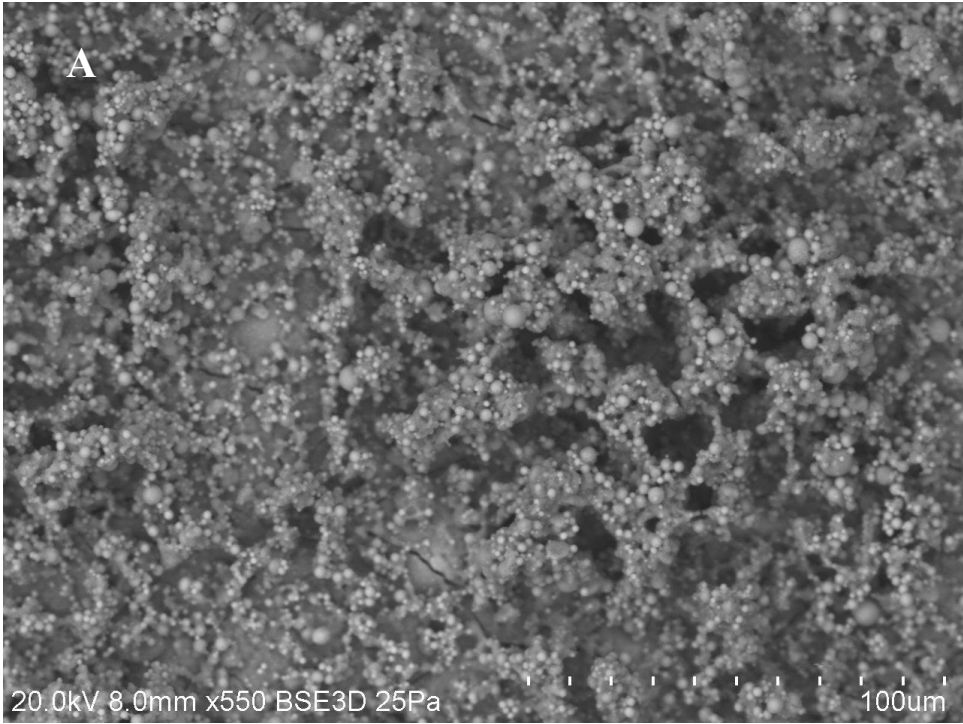


Figure 8: SEM images of hydroxyapatite-titania coated 316 L stainless steel (A) before and (B) after the tape test.